SLAC – PUB – 3746
August 1985
(T/E)

Z DECAYS TO TOP QUARKS*

J. H. KÜHN

CERN, CH-1211 Geneva 23, Switzerland

and

A. REITER†

Stanford Linear Accelerator Center
Stanford University, Stanford, California, 94305

and

P. M. ZERWAS‡

Institute for Theoretical Physics
University of California, Santa Barbara, California 93106
and
Stanford Linear Accelerator Center
Stanford University, Stanford, California 94305

Submitted to *Nuclear Physics B*

---

* Work supported in part by the Department of Energy, contract DE-AC03-76SF00515, and the West German Science Foundation DFG.

† Max Kade Fellow.

‡ Permanent address: Technische Hochschule Aachen, D-5100 Aachen, West Germany

ABSTRACT

Z decays to top quark pairs—if kinematically possible—will provide an accurate measurement of the top quark mass in e^+e^- collisions. We study various distributions of leptons and jets in the final state for semileptonic quark decays. Fragmentation and polarization effects are analyzed. In addition to large longitudinal and transverse polarizations, a small normal t-quark polarization is built up by γ, Z interference and perturbative QCD corrections. We comment also briefly on polarization effects in the $t\bar{b}$ decays of W bosons that are hadronically produced.

1. Introduction

The top quark has been searched for in many experiments in recent years and a lower bound on its mass of 23 GeV has been firmly established. A few prompt, isolated lepton events observed in proton-antiproton collisions are compatible, on the other hand, with the expected signatures of top decays in the mass range between 30 and 50 GeV.[1] Accumulating statistics and a better understanding of the systematics are necessary to strengthen the evidence and to narrow the error margin of the mass value. However, the hadronic environment in which the top quarks are produced and which is theoretically not well under control, will presumably set a limit of several GeV to the accuracy that can finally be reached. In e^+e^- collisions the accuracy should be substantially improved by the analysis of Z decays to top quarks—if they are kinematically possible. An uncertainty of the order of one to two GeV (or even less?) can reasonably be expected from experiments at SLC and LEP before toponium physics will provide the ultimate answer, see Ref. [2] and references quoted therein.

Depending on the detector design, several strategies can be pursued in parallel to measure the properties of top quarks: (i) The branching ratio of $Z \to t\bar{t}$ depends sensitively on the top quark mass m_t for $m_t \lesssim m_Z/2$. Lowest order perturbative QCD corrections,[3] however, change the value predicted by the parton model dramatically leaving us with uncertainties from higher order corrections. (ii) Energy distributions and correlations of leptons and jets in events in which one top quark or both decay semileptonically $t \to b\ell\nu_e$, are strongly affected by the quark mass. (iii) The dominant decay modes of top quarks are decays into 3 jets $t \to bu\bar{d}$, $bc\bar{s}$ of average energy $\sim$ 13 GeV for $m_t \sim 40$ GeV, the central value indicated in the top quark search of Ref. [1]. Reconstruction of these jets will produce mass peaks—a model independent way, in principle, to measure the top mass.[4] Events in which one quark decays semileptonically, may also be of interest in this context since only 4 jets have to be reconstructed, easing the combinatorial problem due to low energy stray hadrons. The method can be ex-

tended to events in which both top quarks decay semileptonically—the cleanest final state possible.

In this paper we will focus our attention on semileptonic top decays. The majority of the distributions is of course also relevant to nonleptonic decays, with leptons and antileptons replaced by quarks and antiquarks appropriately. First we shall study these decays in the parton model (Section 2). Since the mass of the t quark is close to $m_Z/2$ we expect only a very small fraction of energy to be lost in the fragmentation process to T mesons and baryons.[5] Likewise the amount of energy radiated off through perturbative gluon emission should be small. Depolarization phenomena in the fragmentation process[6] introduce some imponderables. We will find nevertheless that lepton spectra and lepton-lepton correlations are sensitive instruments to measure the top quark mass very accurately.

The second part of the paper (Section 3) is devoted to a comprehensive discussion of the t-quark polarization P_N normal to the production plane. This component is generated by γ, Z interference[7,8] and the absorptive part of the QCD corrected $Zt\bar{t}$ vertex. The magnitude and relative size of these two contributions depends on the longitudinal beam polarization. Only for longitudinally polarized beams is P_N found to be large. For unpolarized beams it amounts to 10% at most and is thus far smaller than the dominant longitudinal component. We conclude this section by adding a few comments on polarization phenomena in $W \to t\bar{b}$ decays, produced in quark-antiquark annihilation of hadron colliders.

2. Lepton Distributions in Semileptonic t Decays

The cross section for observing a top quark at the polar angle θ in $e^+e^- \to Z \to t\bar{t}$ [γ exchange near Z neglected] is given by

$$\frac{d\sigma}{d\Omega} = \frac{3\beta}{64\pi^2} \frac{(G_F m_Z^2/2\sqrt{2})^2 Q^2}{[Q^2 - m_Z^2]^2 + [m_Z \Gamma_Z]^2} (v_e^2 + a_e^2)\, \mathcal{N} \tag{1a}$$

$$\mathcal{N} = (v_t^2 + a_t^2)\beta^2(1 + \cos^2\theta) + 2v_t^2(1 - \beta^2) \tag{1b}$$

$$+ 4r_e v_t a_t \beta \cos\theta \ .$$

$\beta = (1 - 4m_t^2/Q^2)^{1/2}$ is the velocity of the quark. The neutral current coupling constants are defined as

$$v_e = -1 + 4\sin^2\theta_w \qquad v_t = 1 - \tfrac{8}{3}\sin^2\theta_w$$
$$a_e = -1 \qquad a_t = 1$$

and

$$r_e = 2v_e a_e/(v_e^2 + a_e^2) \ .$$

The complete, general cross section including beam polarization and quark spins is presented in Appendix A.

Branching ratio $Z \to t\bar{t}$

The partial width $\Gamma(Z \to t\bar{t})$ in the parton model can easily be derived from Eq. (1),

$$\Gamma(Z \to t\bar{t}) = \frac{1}{8\pi} \frac{G_F m_Z^2}{\sqrt{2}} \beta \left[v_t^2 \frac{3 - \beta^2}{2} + a_t^2 \beta^2 \right] \ . \tag{2}$$

Radiative QCD corrections alter the coefficients of the vector and axial vector couplings differently,[2]

$$\frac{3 - \beta^2}{2} \to \frac{3 - \beta^2}{2} \left\{ 1 + \frac{4}{3}\alpha_s \left[\frac{\pi}{2\beta} - \frac{3 + \beta}{4} \left(\frac{\pi}{2} - \frac{3}{4\pi} \right) \right] \right\} \tag{3a}$$

$$\beta^2 \to \beta^2 \left\{ 1 + \frac{4}{3}\,\alpha_s \left[\frac{\pi}{2\beta} - \left(\frac{19}{10} - \frac{22\beta}{5} + \frac{7\beta^2}{2} \right) \left(\frac{\pi}{2} - \frac{3}{4\pi} \right) \right] \right\} . \quad (3b)$$

The QCD coupling constant may be chosen as

$$\alpha_s = \frac{12\pi}{25 \log 4p_t^2/\Lambda^2}$$

with $p_t = \beta m_Z/2$ and $\Lambda \approx 200$ MeV. These QCD corrections introduce a significant deviation of the branching ratio $B(Z \to t\bar{t})$ from the parton model value if m_t approaches $m_Z/2$, as shown in Fig. 1. It has been demonstrated that the QCD corrected cross section coincides very well with the production cross section for $(t\bar{t})$ resonances when averaged over $\gtrsim 100$ MeV energy bins.[9] We can thus be confident that the general characteristics of the mass dependence of the branching ratio are adequately described by Eq. (3) though additional higher order corrections jeopardize a precision measurement of the top-quark mass by this method. One might hope nevertheless that the potentially large higher order corrections sum up to modify the leading term only by a factor $(1 - \exp(-2\pi\alpha_s/3\beta))$ similar to the result in QED.

t-quark polarization

The top quarks are produced in e^+e^--annihilation with a high degree of polarization that affects the distribution of jets and leptons after the decay.[6-8] Neglecting γ, Z interference and QCD loop corrections the polarization vector lies in the t production plane. [The small normal component will be discussed in the next section.] The longitudinal component is large for m_t not too close to $m_Z/2$ and slowly varying with θ,

$$P_L = - \frac{2v_t a_t \beta(1 + \cos^2\theta) + 2r_e(v_t^2 + a_t^2\beta^2)\cos\theta}{(v_t^2 + a_t^2)\beta^2(1 + \cos^2\theta) + 2v_t^2(1 - \beta^2) + 4r_e v_t a_t \beta \cos\theta} . \quad (4a)$$

The transverse polarization, by contrast, has a strong forward-backward asym-

metry,

$$P_\perp = \frac{m_t}{m_Z} \frac{4\sin\theta(v_t a_t \beta\cos\theta + r_e a_t^2)}{(v_t^2+a_t^2)\beta^2(1+\cos^2\theta) + 2v_t^2(1-\beta^2) + 4r_e v_t a_t \beta\cos\theta} \,. \qquad (4b)$$

Both components are displayed in Fig. 2, for a top quark mass of 40 GeV. Averaged over the polar angle, the transverse polarization is very small while the longitudinal polarization is large and negative,

$$\langle P_L\rangle = -\frac{2v_t a_t \beta}{(v_t^2+a_t^2)\beta^2 + \frac{3}{2}\, v_t^2(1-\beta^2)} \qquad (5a)$$

$$\langle P_\perp\rangle = \frac{3\pi}{4}\,\frac{m_t}{m_Z}\, r_e \,\frac{v_t^2}{(v_t^2+a_t^2)\beta^2 + \frac{3}{2}\, v_t^2(1-\beta^2)} \,. \qquad (5b)$$

The measurement of final state correlations among leptons and jets requires the knowledge of spin-spin correlations between t and $\bar{t}$. Dropping terms $\propto v_e a_e/(v_e^2+a_e^2) \leq 10\%$ [they become irrelevant anyway when charges in the final state are summed—this will be assumed from now on for the sake of simplicity], the coefficients of the spin terms in the cross section

$$\frac{d\sigma(s,\bar{s})}{d\Omega} = \frac{d\sigma}{d\Omega}\,\frac{1}{4}\left[1 + b_\mu s_\mu + \bar{b}_\mu \bar{s}_\mu + b_{\mu\nu} s_\mu \bar{s}_\nu\right] \qquad (6)$$

are given as

$$b_\mu = -\frac{4m_t}{Q^2}\, v_t a_t [(1-\beta\cos\theta)k_\mu + (1+\beta\cos\theta)k'_\mu]/\mathcal{N} \qquad (7a)$$

$$\bar{b}_\mu = +\frac{4m_t}{Q^2}\, v_t a_t [(1+\beta\cos\theta)k_\mu + (1-\beta\cos\theta)k'_\mu]/\mathcal{N} \qquad (7b)$$

$$b_{\mu\nu} = [(v_t^2-a_t^2)\beta^2(1-\cos^2\theta)\, g_{\mu\nu} - 4(v_t^2-\beta^2 a_t^2)(k_\mu k'_\nu + k_\nu k'_\mu)/Q^2 \qquad (7c)$$

$$- 4(v_t^2-a_t^2)\beta\cos\theta(k_\mu k'_\nu - k_\nu k'_\mu)/Q^2]/\mathcal{N} \,.$$

k_μ and k'_μ denote the 4-momenta of the initial state electron and positron, respectively (metric $+---$). Orthogonalization with respect to the quark momentum may be carried out if necessary.

QCD corrections have been proved to be large for the width $\Gamma(Z \to t\bar{t}(g))$ whereas angular distributions of the top quarks are only slightly affected. This is a consequence of the fact that the relevant gluon states have small energies so that they cannot alter the direction of heavy quarks. QCD corrected distributions deviate typically less than $\sim 7\%$ from their parton values.[3]* Since heavy quark spins are not flipped by emission of low energy gluons, QCD corrections to the longitudinal and transverse polarization components will also be very small. [This point will be made quantitative in a forthcoming paper]. We therefore can safely neglect all perturbative QCD corrections in the present context.

Fragmentation

In view of the large mass of the top quark it is generally anticipated that almost all the original top quark energy will reside in the top meson or baryon after fragmentation.[5,10] This can be made transparent by analyzing the space-time development of the fragmentation process. The mass difference between the top quark and a $(t\bar{q})$ bound state was estimated in potential models[2] to be $m(t\bar{q}) - m_t \approx 400$ MeV. In the t-quark's rest frame the time $\tau_* \sim \frac{1}{2} fm$ is therefore needed to complete the binding process. In the laboratory frame the t-quark (mass 40 GeV) has then traveled a distance $d \approx \beta\gamma\tau_* \sim \frac{1}{2} fm$ from the center so that a flux tube of length $\sim 1\, fm$ is stretched between t and $\bar{t}$. Assuming an energy density of 1 GeV/fm in the flux tube, just enough field energy has been accumulated to build up two top hadrons—and hardly anything else! Z bosons are therefore expected to decay into a pair of top hadrons of momentum $\beta m_Z/2 \sim 20$ GeV plus at most a few pions† of very low energy $O(1 \text{ GeV})$.* A convenient parametrization of the spectrum is provided by the

---

* This applies also to forward-backward asymmetries which were not plotted correctly in Ref. 3.

† These stray particles must balance angular momentum if the angular distribution of almost exclusively produced pseudoscalar top mesons should coincide with the original quark distribution.

* The energy loss through perturbative gluon bremsstrahlung is similarly small, see Ref. 11. Exclusive channels are discussed in the framework of perturbative QCD in Ref. 12.

fragmentation function[5]

$$D_t(z) \approx \frac{4\sqrt{\epsilon_t}/\pi}{z\left[1-\frac{1}{z}-\frac{\epsilon_t}{1-z}\right]^2} \qquad \epsilon_t \approx 0.15(m_c/m_t)^2 \ . \tag{8}$$

To assess the uncertainties introduced by the fragmentation process, we have varied ϵ_t between 0 and 10^{-3}. If not stated otherwise a value of 10^{-4} was employed. This corresponds to an average energy loss of $\sqrt{\epsilon_t} m_Z/2 \approx 500$ MeV.

Fragmentation reduces the initial t quark polarization quite dramatically. We shall assume that a polarized t quark with $S_z = +\frac{1}{2}$ will convert into $T^*(S_z = 1)$, $T^*(S_z = 0)$, $T^*(S_z = -1)$ and $T(S = 0)$ with relative weight 2:1:0:1.‡ Angular distributions of decay products from $T^*(S_z = +1)$ will be identical to those from $t(S_z = +\frac{1}{2})$ whereas the others will be isotropic.[6] Hence a fraction $f \sim 50\%$ of the t quarks will remain polarized after fragmentation while the others are depolarized.

Top-quark decay

A fraction 2/3 of top quarks with mass $\sim$ 40 GeV will decay into three jets $t \to bu\bar{d}$ and $bc\bar{s}$ (up to radiative QCD corrections), 1/9 to $t \to be^+\nu_e$, μ and τ each. The decay rate for a polarized t quark is described by

$$d\Gamma(s) = d\Gamma[1 + c_\mu s_\mu] \tag{9a}$$

where

$$d\Gamma = \frac{G_F^2 m_t^5}{128\pi^4} \frac{x_\ell\left[1 - x_\ell - \left(\frac{m_b}{m_W}\right)^2\right]}{\left[1 - \left(\frac{m_b}{m_W}\right)^2 - \left(\frac{m_t}{m_W}\right)^2 (1 - x_b)\right]^2} dx_\ell dx_b d\Omega_\ell \tag{9b}$$

‡ T and T^* both decay weakly.[13]

is the width for unpolarized t decay $t \to b\ell^+\nu_\ell$, and the vector

$$c_\mu = -\frac{1}{m_t/2}\left[\frac{1}{x_\ell}\, p_{\ell\mu} - \frac{1}{2}\, p_{t\mu}\right] \tag{9c}$$

has been chosen purely spacelike in the t rest frame; x_i are the energies of b and the charged lepton in units of $m_t/2$. For $\bar{t}$ decays,

$$\bar{c}_\mu = +\frac{1}{m_t/2}\left[\frac{1}{x_\ell}\, p_{\ell\mu} - \frac{1}{2}\, p_{t\mu}\right] \tag{9d}$$

while $d\Gamma$ remains the same.

Lepton and jet distributions

Final state distributions in $e^+e^- \to Z \to t\bar{t}$ after $t, \bar{t}$ fragmentation and decay are generated from a mixture of cross sections in which both top quarks are depolarized, t or $\bar{t}$ is depolarized, or no quark is depolarized. The corresponding probabilities are $(1-f)^2$, $f(1-f)$ and f^2, respectively. This can be summarized as

$$d\sigma_{\text{final}} \propto d\sigma\, D_t D_{\bar{t}} \left\{1 - f[b_\mu c_\mu + \bar{b}_\mu \bar{c}_\mu] + f^2 b_{\mu\nu} c_\mu \bar{c}_\nu\right\}\, d\Gamma(t)\, d\Gamma(\bar{t})\ . \tag{10}$$

We shall now discuss in detail some distributions that are relevant to measurements of the top quark mass.

Leptons originating form top quark decays can be experimentally distinguished from prompt secondary leptons that are decay products of bottom or charm quarks, by defining an isolation criterion which forbids the lepton to be close to any of the jets in the final state. In Fig. 3 we investigate how this charged lepton spectrum depends on fragmentation and polarization parameters. We illustrate the results by choosing two top quark masses, $m_t = 37.5$ GeV and 42.5 GeV. In Fig. 3a the shape of the spectrum does not vary much if ϵ_t is restricted to a reasonable range $\leq 10^{-3}$. The depolarization mechanism introduces a larger change in the distributions as is evident from Fig. 3b where f is varied between

0 and 1. Note that the shape of this spectrum is up to $\mathcal{O}(\epsilon_t)$ described by[6]

$$\frac{dN}{d\left(\frac{2E_\ell}{m_Z}\right)}$$

$$= \begin{cases} 32\left(\frac{2E_\ell}{m_Z}\right)^2\gamma^4\left[3-2\frac{2E_\ell}{m_Z}\gamma^2(3+\beta^2)\right]+f\langle P_L\rangle\beta\left(-3+8\gamma^2\frac{2E_\ell}{m_Z}\right) \\ \qquad \text{for } 0<\frac{2E_\ell}{m_Z}<\frac{1}{2}(1-\beta) \\ \frac{2}{\beta}(1-\xi)^2\left[(1+2\xi)-f\frac{\langle P_L\rangle}{\beta}(1-\xi-3\beta\xi)\right] \\ \qquad \text{for } \frac{1}{2}(1-\beta)<\frac{2E_\ell}{m_Z}<\frac{1}{2}(1+\beta) \end{cases} \tag{11}$$

where $\xi = \frac{2E_\ell}{m_Z}\Big/\frac{1}{2}(1+\beta)$. The width of the band would limit the accuracy of a measurement of the t mass to roughly 2 GeV. However, if a value $f \approx \frac{1}{2}$ is adopted, as suggested above, the uncertainty is reduced to less than $\sim$ 1 GeV. [Note that f can be studied independently in lepton-antilepton correlations as explained in Eq. (10).] This is summarized in Fig. 3c where ϵ_t is allowed to vary between 10^{-4} and 10^{-3}, and f between 1/3 and 2/3. Neutrino and jet energy distributions are shown in Fig. 4 for $\epsilon_t = 10^{-4}$ and $f = \frac{1}{2}$.*

Prompt charged leptons and neutrinos are copiously produced in the decay chains $t \to b \to c \to s$ and $\bar{t}$ correspondingly. Assuming a non-leptonic branching ratio for c-quark decays of $\sim$ 80%, for b-quark decays of $\sim$ 60% (including secondaries) and for primordial t quark decays of 70% we find that only $\sim$ 15% of $t\bar{t}$ decay events are nonleptonic, and only $\sim$ 35% don't have any leptonic secondaries. Some more details are given in Table 1. Secondary leptons have a much softer spectrum than primordial leptonic decays. The electron/muon spectrum and the distribution of neutrino energy due to secondary lepton decays are displayed in Fig. 5. A cut of $\sim$ 5 GeV in the lepton energy reduces the number of

* We approximate the invariant b-jet mass by its quark mass value $m_b = 5$ GeV.[14]

these events quite efficiently while not affecting the primary signal very much. This cut together with the isolation criterion should give us a clear sample of primary semileptonic t decay events.

A lovely class consists of events in which both t and $\bar{t}$ decay semileptonically,

$$e^+e^- \to Z \to t\bar{t} \begin{cases} \to \bar{b}\ell^-\bar{\nu}_\ell \\ \to b\ell^+\nu_\ell \end{cases} .$$

The final state contains two isolated leptons plus two jets, all with an average energy of $\sim$ 12 GeV and well separated so that the jets should be easy to reconstruct. In Fig. 6a we show the energy distribution of the charged leptons in these events, in Fig. 6b the jet energy. The distribution of the total neutrino energy and the neutrino momentum are displayed in Fig. 6c. Finally in Fig. 6d we present the distribution of the invariant mass of charged lepton pairs. Such events will be promising candidates for an accurate measurement of the top quark mass.

Even though two non-parallel neutrinos are among the final particles, a few clean events of this class allow us to reconstruct the top-quark mass very nicely. Missing energy and momentum define the 4-momentum vector $K = k_\nu + k_{\overline{\nu}}$. Boosting the event into the rest frame of K, it is clear that the angular direction of $\vec{k}_\nu = -\vec{k}_{\overline{\nu}}$ in this frame is arbitrary. The condition that the two masses reconstructed from the two sets {jet + lepton + neutrino} in an event must coincide, leaves us with a 1-dimensional manifold of solutions for the t mass. Doing this repeatedly for a number of events the reconstructed masses cluster quickly at the true top quark mass. This is shown for $N = 100$ Monte Carlo events in Fig. 7 with an initial t mass $m_t = 40$ GeV. [We employed a 9×36 grid in θ_ν and ψ_ν to cover the unit sphere of the neutrino directions, and we required the 2 masses to coincide within a difference of 1 GeV.] Particle losses in detectors can be corrected for on a statistical basis by Monte Carlo simulations.

3. Normal t-Quark Polarization

We have argued that top quarks are produced with a high degree of polarization in e^+e^- collisions. For the dominating mechanism $e^+e^- \to Z \to t\bar{t}$ the polarization vector lies in the production plane spanned by the momentum vectors of e^- and t. The nonvanishing correlations $\vec{s}\cdot\vec{n}_{e^-}$ and $\vec{s}\cdot\vec{n}_t$ between spin and momentum vectors reflect the parity violation of the neutral current interactions. A normal component of the polarization vector (parallel to $\vec{n}_{e^-}\times\vec{n}_t$) is, on the other hand, odd under a time reversal transformation. Such a polarization state can be generated by violation of time reversal invariance as well as interference effects between various production amplitudes. While the standard model does not allow for breaking of time reversal invariance in diagonal neutral current interactions, interference between non-real Z exchange and real γ exchange amplitudes,[7,8] and between Born amplitudes and non-real vertex QCD corrections (perturbative final state interactions) will generate a finite normal polarization of the t quark. These terms (and only these) will lead to parity/charge conjugation odd terms in the lepton distributions after t decay.* For energies close to the Z mass the γ amplitude is small compared to the Z amplitude. We therefore expect QCD loop corrections of the Z amplitude to be as important as γ, Z interference, Fig. 8a-c,

$$P_N = P_N(\gamma Z) + P_N(QCD)\ . \tag{12}$$

The contribution to P_N due to γ, Z interference is easily evaluated. In the same notation as used in the preceding section, we find

$$P_N(\gamma Z) = -\frac{16\pi\alpha}{G_F m_Z^2/2\sqrt{2}}\ \frac{m_Z\Gamma_Z}{Q^2}\ \frac{m_t}{\sqrt{Q^2}}\ \beta\sin\theta[e_e a_e e_t a_t]/\mathcal{N}\ . \tag{13}$$

The normalization $\mathcal{N}$ is defined in Eq. (1b), and $e_e = -1$, $e_t = 2/3$ are the charges of electron and top quark. As anticipated, the normal polarization is

* Note that $P_{L,\perp}(\bar{t}) = -P_{L,\perp}(t)$ but $P_N(\bar{t}) = +P_N(t)$.

a consequence of the relative phase between the γ and the Z propagator, $\propto \mathrm{Im}(1/Q^2 \cdot 1/[Q^2 - m_Z^2 + im_Z\Gamma_Z])$, non-real due to the finite width of Z.

The QCD vertex correction in Fig. 8c alters the top quark current $\gamma_\mu(v_t - a_t\gamma_5)$. As we are only interested in the absorptive, infrared finite part of the form factors, this amounts to the substitutions

$$\gamma_\mu \Rightarrow \gamma_\mu[1 + i\mathrm{Im}f] - \frac{p_\mu}{m_t}\, i\mathrm{Im}f \tag{14a}$$

$$\gamma_\mu\gamma_5 \Rightarrow \gamma_\mu\gamma_5[1 - i\mathrm{Im}f] \; . \tag{14b}$$

p_μ is the 4-momentum of the top quark. The absorptive part of the magnetic form factor[3]

$$\mathrm{Im}f = \frac{4\alpha_s}{3}\,\frac{m_t^2}{Q^2}\,\frac{1}{\beta} \tag{15}$$

shows the characteristic β^{-1} singularity at threshold [this gives rise to the large QCD correction of the $Z \to t\bar{t}$ width, rendered finite only by shrinking phase space $\propto \beta$]. The resulting polarization can be written as†

$$P_N(QCD) = -\frac{4\alpha_s}{3}\,\frac{m_t}{\sqrt{Q^2}}\sin\theta[(v_e^2 + a_e^2)v_t^2\beta\cos\theta + 2v_e a_e v_t a_t(2 - \beta^2)]/\mathcal{N} \; . \tag{16}$$

Before evaluating these expressions numerically, it should be pointed out that they can easily be generalized for the case of longitudinally polarized electrons and positrons by substituting

$$e_e e_t\,\frac{a_e a_t}{v_e^2 + a_e^2} \to e_e e_t\,\frac{(\rho v_e + a_e)a_t}{(v_e^2 + a_e^2) + 2\rho v_e a_e}$$

$$v_t a_t\,\frac{2v_e a_e}{v_e^2 + a_e^2} \to v_t a_t\,\frac{v_e(a_e + \rho v_e) + (v_e + \rho a_e)a_e}{(v_e^2 + a_e^2) + 2\rho v_e a_e}$$

where ρ is given in terms of electron and positron polarizations π_- and π_+ by $\rho = (\pi_+ - \pi_-)/(1 - \pi_+\pi_-)$. $P_N(\gamma Z)$ and P_N (QCD) are dramatically enhanced

† Replacing the weak charges by the electric charges, this expression approaches the formula of Ref. 15 in the relativistic limit.

for longitudinally polarized beams—albeit in angular regions of small production rate. For $\rho = +1$ the two contributions act cumulatively, for $\rho = -1$ they nearly cancel (Fig. 9).

The preceding discussion of polarization phenomena applies equally well to $Z \rightarrow t\bar{t}$ produced in colliding quark beams of hadron machines. In addition to Fig. 8c, two more QCD diagrams could in principle contribute to the normal polarization. However, the infrared finite, absorptive part of the light-quark form factor vanishes for $m_q \rightarrow 0$, as evident from Eq. (15). The box diagram in which Z and a gluon propagate parallel $q\bar{q} \rightarrow Z + g \rightarrow t\bar{t}$, does not interfere with the Born term since the quarks in the former diagram are in a color octet state while being in a color singlet state in the latter diagrams. The t polarization vector thus follows form the previous formulae by the appropriate substitutions of the electroweak charges.

The same procedure can be followed for t decays from W bosons produced in quark-antiquark collisions, $u\bar{d} \rightarrow W^+ \rightarrow t\bar{b}$. If the b quark mass is neglected, the effective, QCD corrected charged quark current can be cast into the form

$$\gamma_\mu(1-\gamma_5) \rightarrow \gamma_\mu(1-\gamma_5) - \frac{2p_\mu}{m_t}\, i\mathrm{Im}f \tag{17}$$

where[16]

$$\mathrm{Im}f = \frac{\alpha_s}{3}\,\frac{m_t^2}{Q^2}\,. \tag{18}$$

Interference between the Born amplitude and QCD vertex correction results in the following normal polarization of the t quark

$$P_N(QCD) = -\,\frac{2\alpha_s}{3}\,\frac{m_t}{\sqrt{Q^2}}\,\frac{\beta\sin\theta}{1+\beta\cos\theta} \tag{19}$$

where θ denotes the angle between u and t quark in the W^+ rest frame. The velocity of the t quark is given by $\beta = (Q^2 - m_t^2)/(Q^2 + m_t^2)$.

Longitudinal and transverse polarization are easily obtained by substituting $p_t \Rightarrow p_t - m_t s_t$ in the spin averaged cross section which is $\propto (p_u p_{\bar{b}})(p_{\bar{d}} p_t)$ in Born approximation,

$$P_L = -\frac{\beta + \cos\theta}{1 + \beta\cos\theta} \tag{20a}$$

$$P_\perp = \frac{\sqrt{1-\beta^2}\sin\theta}{1 + \beta\cos\theta} \,. \tag{20b}$$

t quarks with mass $m_t \approx m_W/2$, i.e. $\beta \approx 3/5$, have large longitudinal and transverse polarizations, as is evident from the average over θ,

$$\langle P_L \rangle = -\beta \tag{21a}$$

$$\langle P_\perp \rangle = \frac{\pi}{4}\sqrt{1-\beta^2} \,. \tag{21b}$$

However, the average normal polarization

$$\langle P_N \rangle = -\frac{\pi\alpha_s}{6}\,\frac{m_t}{\sqrt{Q^2}}\,\beta$$

is rather small for all mass values.

4. Conclusion

Semileptonic decays of top quarks which presumably can be studied in Z decays at SLC and LEP, allow a determination of the top quark mass with an accuracy of 1-2 GeV if $m_t \sim 40$ GeV. Energy distributions of leptons and jets in semileptonic decays as well as correlations between the two leptons in events where the t and $\bar{t}$-quark both decay semileptonically, turn out to be strongly affected by the mass of the top quark. Uncertainties due to fragmentation and polarization effects will restrict measurements of m_t to the error margin discussed above.

ACKNOWLEDGEMENTS

We have benefitted from discussions with J. Dorfan, B. Harms, B. Hollebeek and F. Richard. Two of us, A.R. and P.Z., are grateful to S. Brodsky and S. Drell for the warm hospitality extended to them in the SLAC Theory Group. P.Z. also thanks S. Brodsky and R. Schrieffer for the invitation to the QCD Workshop.

APPENDIX A

The general matrix element for the production of t and $\bar{t}$ quarks in e^+e^- annihilation involving vector and axial vector currents can be written as

$$T = \frac{e^2}{s} \sum_{i,k} Z_{ik} \cdot \bar{u}(t)\gamma_5^i \gamma_\mu v(\bar{t}) \cdot \bar{v}(e^+)\gamma_5^k \gamma^\mu u(e^-) \ , \tag{A1}$$

$i, k = 0(1)$ standing for vector (axial vector) couplings. [The discussion closely follows Ref. 17.]

We allow for longitudinally polarized electron and positron beams of polarization degree π_- and π_+ respectively. The differential cross section is then given by

$$\frac{d\sigma}{d\Omega} = \frac{\alpha^2 \beta}{4s} \sum |T|^2$$

$$\begin{aligned} \sum |T|^2 = \frac{1 - \pi_+\pi_-}{s^2} \frac{1}{2} \Big[& D_V (F_+^1 - F_+^3) + D_A (F_+^1 + F_+^3) + 2\mathrm{Re}\, D_{VA} F_+^2 \\ & + 2\mathrm{Im}\, D_{VA} F_+^4 + E_V (F_-^1 - F_-^3) + E_A (F_-^1 + F_-^3) \\ & + 2\mathrm{Re}\, E_{VA} F_-^2 + 2\mathrm{Im}\, E_{VA} F_-^4 \Big] \ . \end{aligned} \tag{A2}$$

D and E are given by a combination of coupling constants and $\rho \equiv (\pi_+ - \pi_-)/(1 - \pi_+\pi_-)$ as follows

$$\begin{aligned} D_V &= |Z_{VV}|^2 + |Z_{AV}|^2 + 2\rho \mathrm{Re}\, Z_{VV} Z_{AV}^* \ , \\ D_A &= |Z_{VA}|^2 + |Z_{AA}|^2 + 2\rho \mathrm{Re}\, Z_{VA} Z_{AA}^* \ , \\ D_{VA} &= Z_{VA} Z_{VV}^* + Z_{AA} Z_{AV}^* + \rho (Z_{VA} Z_{AV}^* + Z_{AA} Z_{VV}^*) \ , \\ E_V &= \rho (|Z_{VV}|^2 + |Z_{AV}|^2) + 2\mathrm{Re}\, Z_{VV} Z_{AV}^* \ , \\ E_A &= \rho (|Z_{VA}|^2 + |Z_{AA}|^2) + 2\mathrm{Re}\, Z_{VA} Z_{AA}^* \ , \\ E_{VA} &= \rho (Z_{VA} Z_{VV}^* + Z_{AA} Z_{AV}^*) + (Z_{VA} Z_{AV}^* + Z_{AA} Z_{VV}^*) \ . \end{aligned} \tag{A3}$$

The $F_{\pm}^{i}$ are functions of the 4-momenta $P \equiv p_{e^-} + p_{e^+}$, $\ell \equiv p_{e^-} - p_{e^+}$, $q \equiv p_t - p_{\bar{t}}$ and of the top quark (antiquark) spin vectors s_+ (s_-).

$$
\begin{aligned}
F_+^1 &= \tfrac{1}{2}\,(s^2 + (\ell q)^2) + 2m^2(\ell s_+ \cdot \ell s_- - P s_+ \cdot P s_-) \\
F_+^2 &= sm(P s_- - P s_+) + m\ell q(-\ell s_- - \ell s_+) \\
F_+^3 &= -2sm^2 + \tfrac{1}{2}\,\left[(\ell q)^2 - s^2 + 4m^2 s\right]\, s_+ s_- \\
&\quad + (s - 2m^2)\,\left[P s_+ \cdot P s_- - \ell s_+ \cdot \ell s_-\right] \\
&\quad - \ell q\,\left[P s_- \cdot \ell s_+ - \ell s_- \cdot P s_+\right] \\
F_+^4 &= -\tfrac{1}{2}\,\left[\ell s_- \epsilon(\ell, P, q, s_+) + \ell s_+ \epsilon(\ell, P, q, s_-) - \ell q \epsilon(\ell, q, s_-, s_+)\right]
\end{aligned}
\qquad (A4)
$$

$$
\begin{aligned}
F_-^1 + F_-^3 &= 2\ell q m[-P s_- + P s_+] \\
F_-^1 - F_-^3 &= 2sm(\ell s_- + \ell s_+) \\
F_-^2 &= -\ell q s - 2m^2(\ell s_- \cdot P s_+ - \ell s_+ \cdot P s_-) \\
F_-^4 &= -m\epsilon(s_+, \ell, q, P) - m\epsilon(s_-, \ell, q, P)\ .
\end{aligned}
$$

In the standard model the constants Z_{ik} are given by

$$
\begin{aligned}
Z_{VV} &= v_e v_t d - e_t \\
Z_{VA} &= v_e a_t d \\
Z_{AV} &= a_e v_t d \\
Z_{AA} &= a_e a_t d \\
d &= \frac{s}{s - m_Z^2 + i m_Z \Gamma_Z}\ \frac{1}{16 \sin\theta_W \cos^2\theta_W}\ ; \\
v_f &= 2I_3^f - 4e_f \sin^2\theta_W\ ; \qquad a_f = 2I_3^f\ .
\end{aligned}
\qquad (A5)
$$

For the constants D and E one finds

$$
\begin{aligned}
D_V &= |d|^2 \left[e_t^2/|d|^2 + (v_e^2 + a_e^2 + 2\rho v_e a_e) v_t^2 - 2 e_t v_t (v_e + \rho a_e) \mathrm{Re}\, 1/d^* \right] \\
D_A &= |d|^2 \left[v_e^2 + a_e^2 + 2\rho v_e a_e \right] \; a_t^2 \\
D_{VA} &= |d|^2 \left[v_t (v_e^2 + a_e^2 + 2\rho v_e a_e) - e_t (v_e + \rho a_e) \; 1/d^* \right] \; a_t \\
E_V &= |d|^2 \left[\rho e_t^2/|d|^2 + (\rho (v_e^2 + a_e^2) + 2 v_e a_e) v_t^2 - 2 e_t v_t (\rho v_e + a_e) \mathrm{Re}\, 1/d^* \right] \\
E_A &= |d|^2 \left[\rho (v_e^2 + a_e^2) + 2 v_e a_e \right] \; a_t^2 \\
E_{VA} &= |d|^2 \left[v_t (\rho (v_e^2 + a_e^2) + 2 v_e a_e) - e_t (\rho v_e + a_e) \, 1/d^* \right] \; a_t \; .
\end{aligned}
\tag{A6}
$$

REFERENCES

1. G. Arnison *et al.*, Phys. Lett. 147B (1984) 493.
2. S. Güsken, J. H. Kühn, and P. M. Zerwas, SLAC-PUB-3580, March 1985.
3. J. Jersak, E. Laermann and P. M. Zerwas, Phys. Rev. D25 (1982) 1218.
4. F. Richard and P. Roudeau, Experience Delphi FR/PR/OM/85/13.
5. C. Peterson, D. Schlatter, I. Schmitt and P. M. Zerwas, Phys. Rev. D27 (1983) 105.
6. J. H. Kühn, Nucl. Phys. B237 (1984) 77.
7. M. Gourdin, Lepton pair production in e^+e^- annihilation processes, PAR-LPTHE 78/17.
8. N. Anselmino, P. Kroll and B. Pire, CERN-TH-4172/85.
9. S. Güsken, J. H. Kühn and P. M. Zerwas, Phys. Lett. 155B (1985) 185.
10. J. D. Bjorken, Phys. Rev. D17 (1978) 171; M. Suzuki, Phys. Lett. 71B (1977) 189.
11. Y. Azimov, Y. Dokshitser, V. Khoze, and S. Troian, Sov. J. Nucl. Phys. 38 (1983) 498.
12. F. Amiri, B. C. Harms, C.-R. Ji, SLAC-PUB-3749 (1985).
13. I. Bigi and H. Krasemann, Z. Phys. C7 (1981) 127.
14. M. Suzuki, Phys. Rev. D31 (1985) 662.
15. A. Devoto, J. Pumplin, W. Repko and G. L. Kane, Phys. Rev. Lett. 43 (1979) 1062.
16. H. D. Tholl, Diploma Thesis, RWTH Aachen, 1985.
17. J. H. Kühn and F. Wagner, Nucl. Phys. B236 (1984) 16.

FIGURE CAPTIONS

1. The branching ratio $B(Z^0 \to t\bar{t})$ in Born approximation and with first order QCD corrections. The shaded area indicates how an uncertainty of 30% of the QCD correction due to higher orders would affect the result.

2. The longitudinal polarization P_L, transverse polarization $P_\perp$ and normal polarization P_N of the top-quarks in $e^+e^- \to t\bar{t}$ on Z^0 for unpolarized beams as functions of the scattering angle θ. (P_N, built up from $\gamma - Z$ interference and higher order QCD corrections and shown here for comparison, is more extensively discussed in Section 3).

3. Energy distribution of the charged lepton in $e^+e^- \to Z^0 \to t\bar{t}$ where only the t or $\bar{t}$-quark decays semileptonically.

   a) Dependence on the fragmentation parameter (no polarization). The result is shown for a top-mass value of $m_t = 42.5$ GeV and ϵ_t varying between 0 and 10^{-3}.

   b) Dependence on polarization effects. Results for 3 different values of the depolarization parameters $f = 0, 0.5, 1$ for a top-quark mass of $m_t = 42.5$ GeV and a fragmentation parameter $\epsilon_t = 10^{-4}$. $f = 0$ indicates complete depolarization, $f = 1$ no depolarization.

   c) Dependence on polarization *and* fragmentation effects for two top-mass values $m_t = 37.5$ GeV and 42.5 GeV. The shaded areas indicate bounds of the energy distribution for depolarization parameters in the expected range $1/3 \leq f \leq 2/3$ and fragmentation parameters in the range $10^{-4} \leq \epsilon_t \leq 10^{-3}$.

4. Distribution of the jet energies (a) and neutrino energies (b) in the process $e^+e^- \to Z^0 \to t\bar{t}$ where only the t or $\bar{t}$-quark decays semileptonically. The results are given for a top-mass value $m_t = 42.5$ GeV, depolarization parameter $f = 0.5$ and fragmentation parameter $\epsilon_t = 10^{-4}$.

5. Energy distribution of prompt charged leptons (e, μ) due to secondary decays and distribution of the missing energy in the process $e^+e^- \to Z^0 \to t\bar{t}$

where the primary t and $\bar{t}$-quark decays are nonleptonic or τ decays (producing the long tail in the neutrino energy distribution). The results are given for the following parameter values: $m_t = 42.5$ GeV, $f = 0.5$, $\epsilon_t = 10^{-4}$.

6. Energy distribution of the two charged leptons (e, μ) (a) and jets (b), distribution of the missing energy and missing momentum (c), and the invariant mass of the charged lepton pairs (d) in the process $e^+e^- \rightarrow Z^0 \rightarrow t\bar{t}$, where the t *and* $\bar{t}$-quark both decay semileptonically. The results are given for top-quark masses $m_t = 37.5$ GeV and $m_t = 42.5$ GeV, depolarization parameter $f = 0.5$ and fragmentation parameter $\epsilon_t = 10^{-4}$.

7. Reconstructed masses of the charged lepton-jet-neutrino systems for a top quark mass $m_t = 42.5$ GeV, depolarization parameters $f = 0$ and fragmentation parameter $\epsilon = 10^{-4}$. The result is given for a 9×36 grid in θ_ν, ψ_ν to cover the unit sphere of the neutrino direction in the $\nu\bar{\nu}$ cms, and allowing a maximal difference of 1 GeV for the 2 reconstructed masses.

8. Feynman diagrams contributing to the normal polarization P_N of the top-quark in $e^+e^- \rightarrow Z^0, \gamma \rightarrow t\bar{t}$.
   a) Z^0-exchange Born graph;
   b) γ-exchange Born graph;
   c) Z^0-exchange including QCD vertex correction.

9. Polarization P_N of the top quark, normal to the production plane in $e^+e^- \rightarrow t\bar{t}$ on the Z^0. The polarization is separately shown for various beam polarizations. The top quark mass was chosen to be 40 GeV. P_N is broken down into contributions from $\gamma - Z$-interference and QCD vertex corrections. The angular dependence of the cross section is indicated by the $- - \cdot\cdot$ lines.

TABLE 1

Probability for observing a given number of prompt e's/μ's and neutrinos in the decay products of t and $\bar{t}$ (including secondary decays) in the process $e^+e^- \to t\bar{t}$.

Charged Leptons	Probability	Neutrinos	Probability
0	0.141	0	0.103
1	0.326	1	0.237
2	0.320	2	0.268
3	0.160	3	0.193
4	0.047	4	0.114
5	0.006	5	0.055
6	0.0003	6	0.020
		7	0.007
		8	0.002
		9	0.0004
		10	0.0002
$\langle \#\ell \rangle = 1.67$		$\langle \#\nu \rangle = 2.27$	

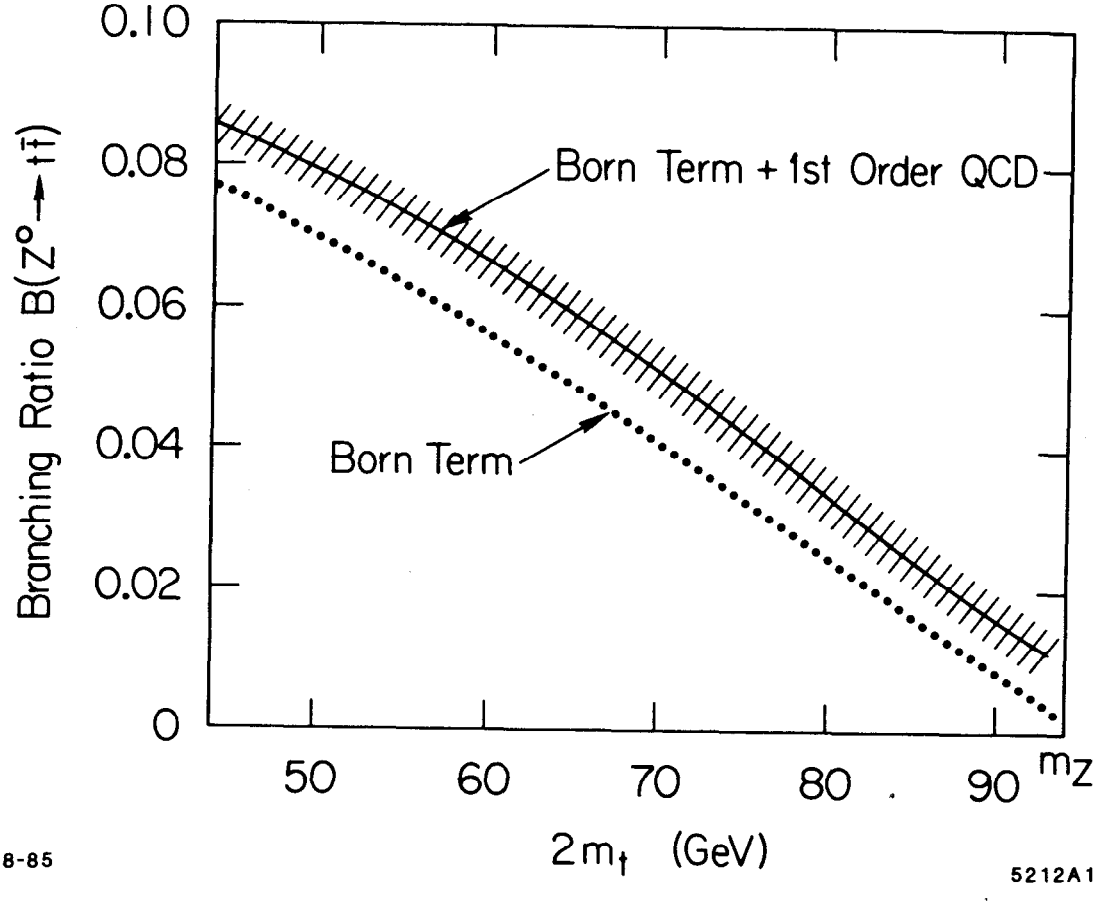
0.10
0.08
0.06
0.04
0.02
0
Branching Ratio B(Z°→ tt̄)
Born Term + 1st Order QCD
Born Term
50
60
70
80
90
mZ
2mt (GeV)
8-85
5212A1

FIG. 1

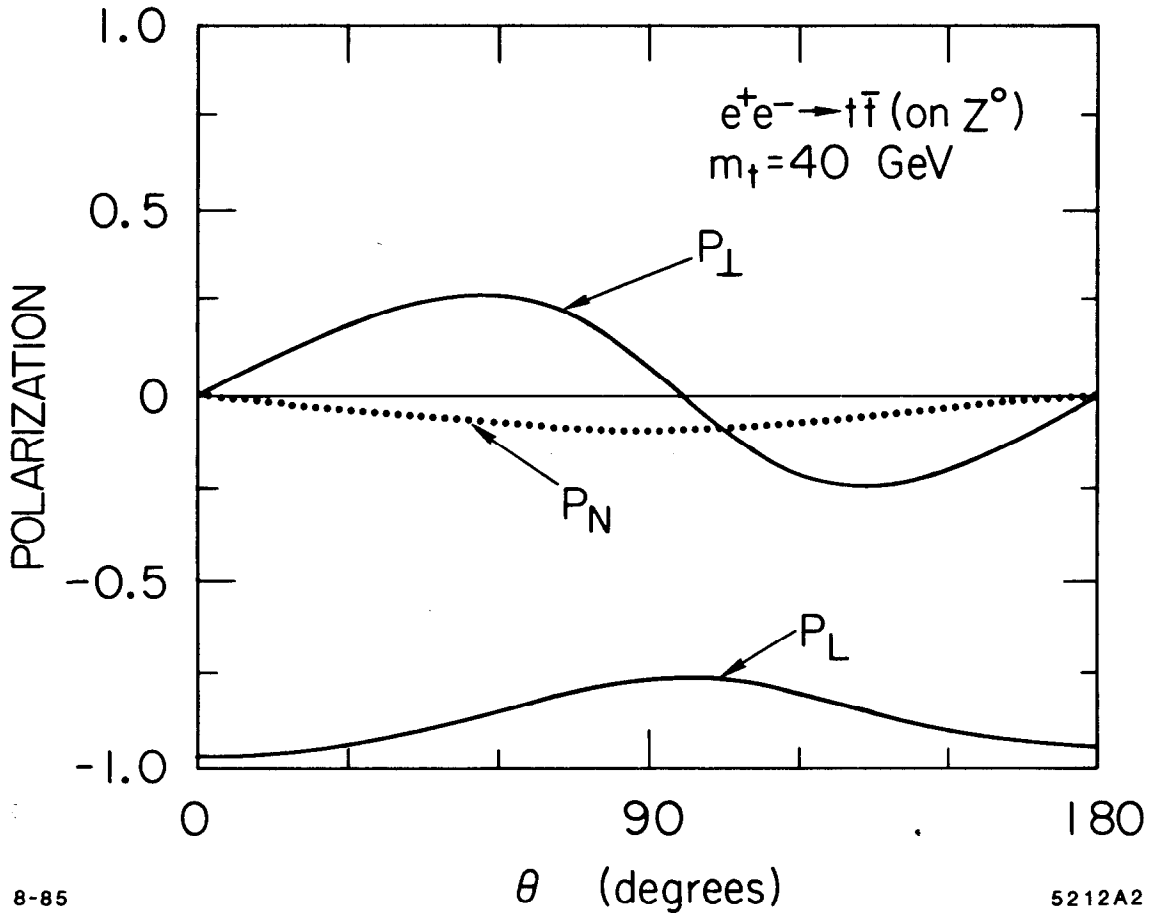
1.0
0.5
0
-0.5
-1.0
POLARIZATION
$e^+e^- \rightarrow t\bar{t}$ (on Z°)
m_t=40 GeV
$P_\perp$
P_N
P_L
0
90
180
θ (degrees)
8-85
5212A2

FIG. 2

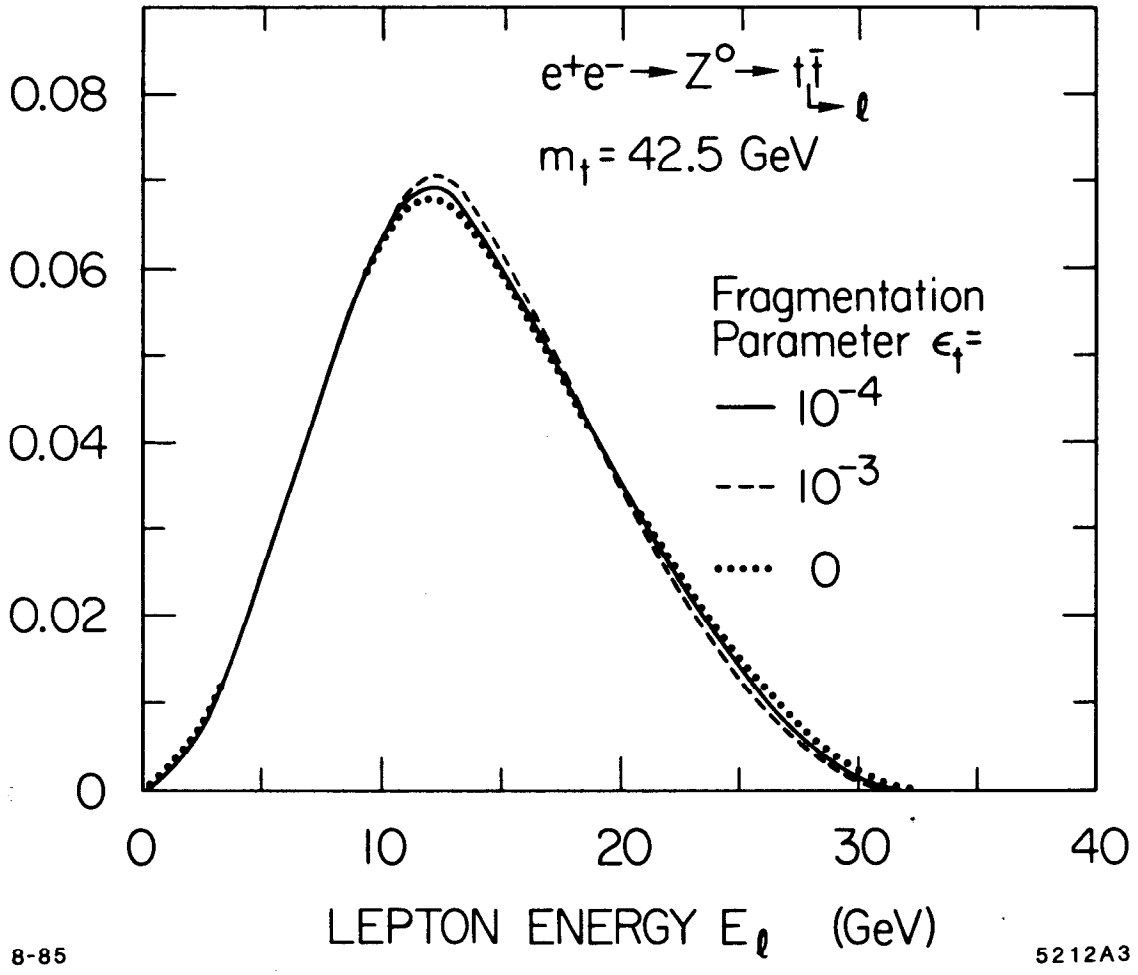
$e^+e^- \rightarrow Z^0 \rightarrow t\bar{t}$
ℓ
$m_t = 42.5$ GeV
Fragmentation Parameter ϵ_t=
10^{-4}
10^{-3}
0
0.08
0.06
0.04
0.02
0
0
10
20
30
40
LEPTON ENERGY E_ℓ (GeV)
8-85
5212A3

FIG. 3A

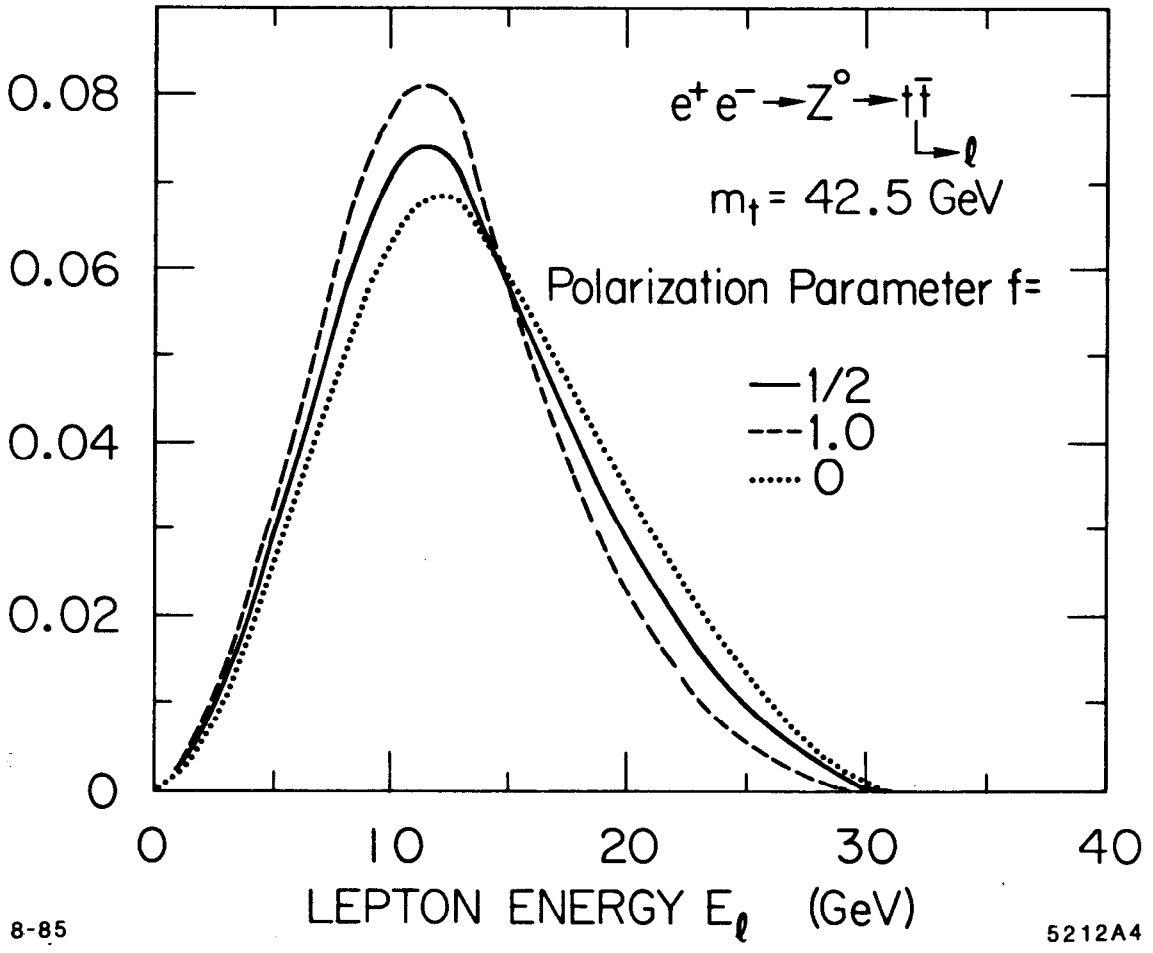
0.08
0.06
0.04
0.02
0
0
10
20
30
40
$e^+e^- \rightarrow Z^\circ \rightarrow t\bar{t}$
$\hookrightarrow \ell$
m_t = 42.5 GeV
Polarization Parameter f=
—1/2
---1.0
..... 0
LEPTON ENERGY E_ℓ (GeV)
8-85
5212A4

FIG. 3B

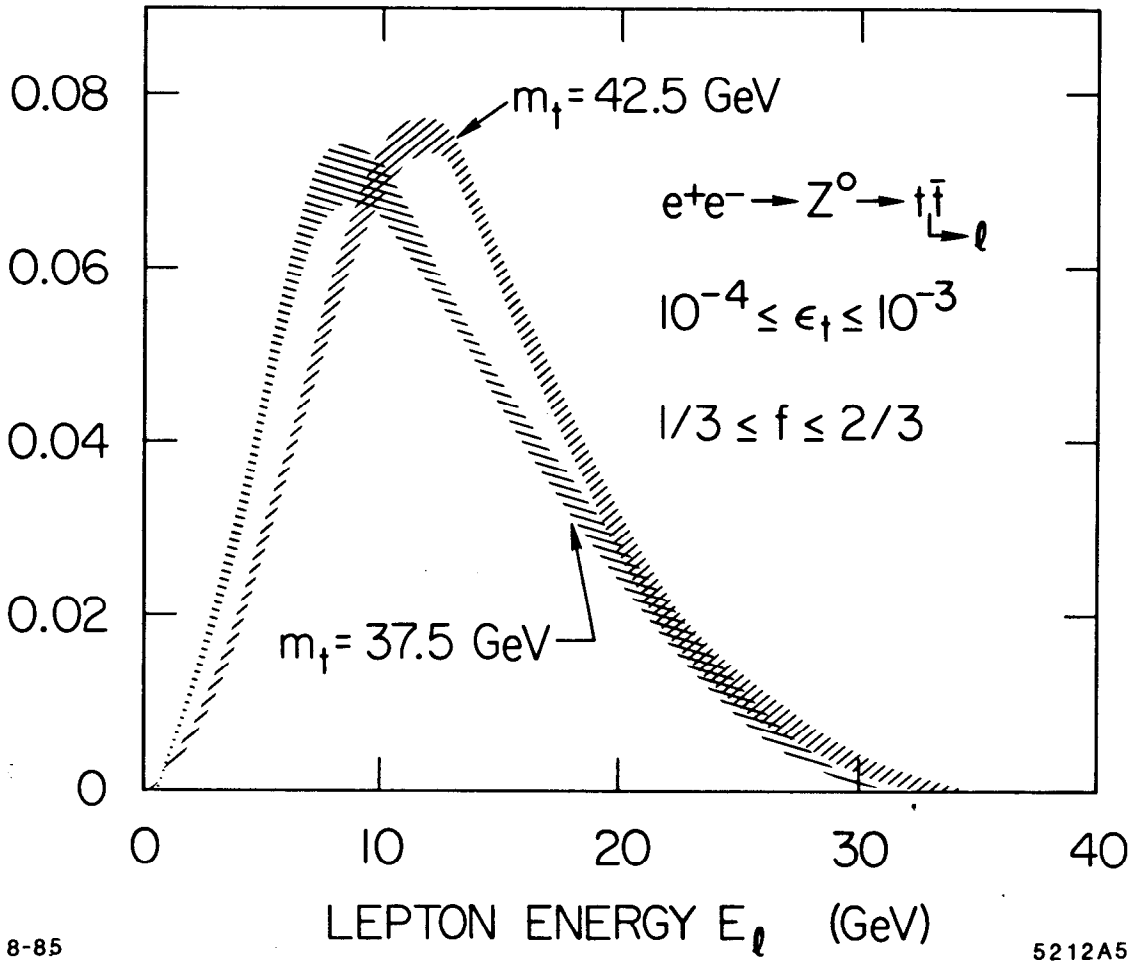
0.08
0.06
0.04
0.02
0
$m_t = 42.5$ GeV
$e^+e^- \rightarrow Z^0 \rightarrow t\bar{t}$
ℓ
$10^{-4} \leq \epsilon_t \leq 10^{-3}$
$1/3 \leq f \leq 2/3$
$m_t = 37.5$ GeV
0
10
20
30
40
LEPTON ENERGY E_ℓ (GeV)
8-85
5212A5

FIG. 3c

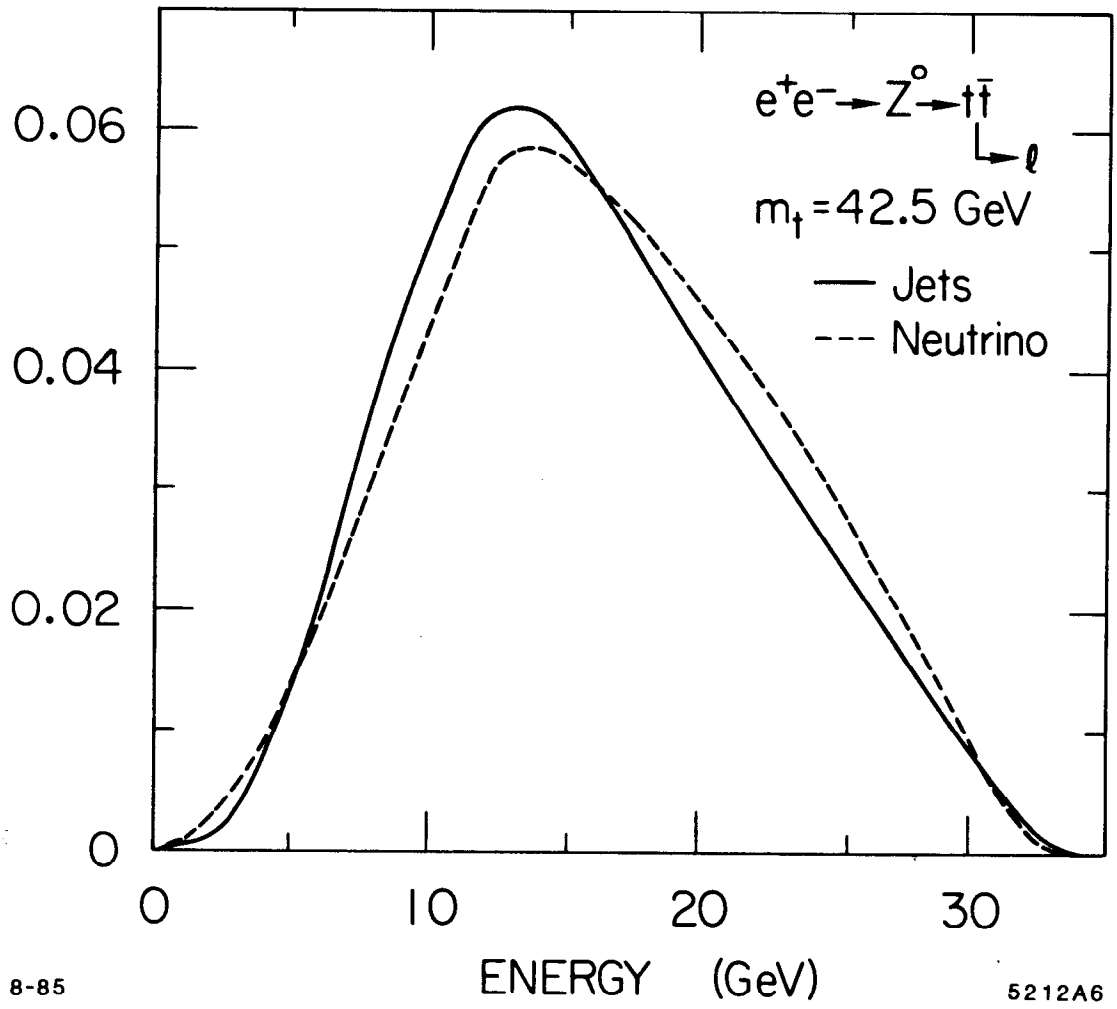
$e^+e^- \rightarrow Z^\circ \rightarrow t\bar{t}$
$\rightarrow \ell$
$m_t = 42.5$ GeV
Jets
Neutrino
0.06
0.04
0.02
0
0
10
20
30
ENERGY (GeV)
8-85
5212A6

FIG. 4

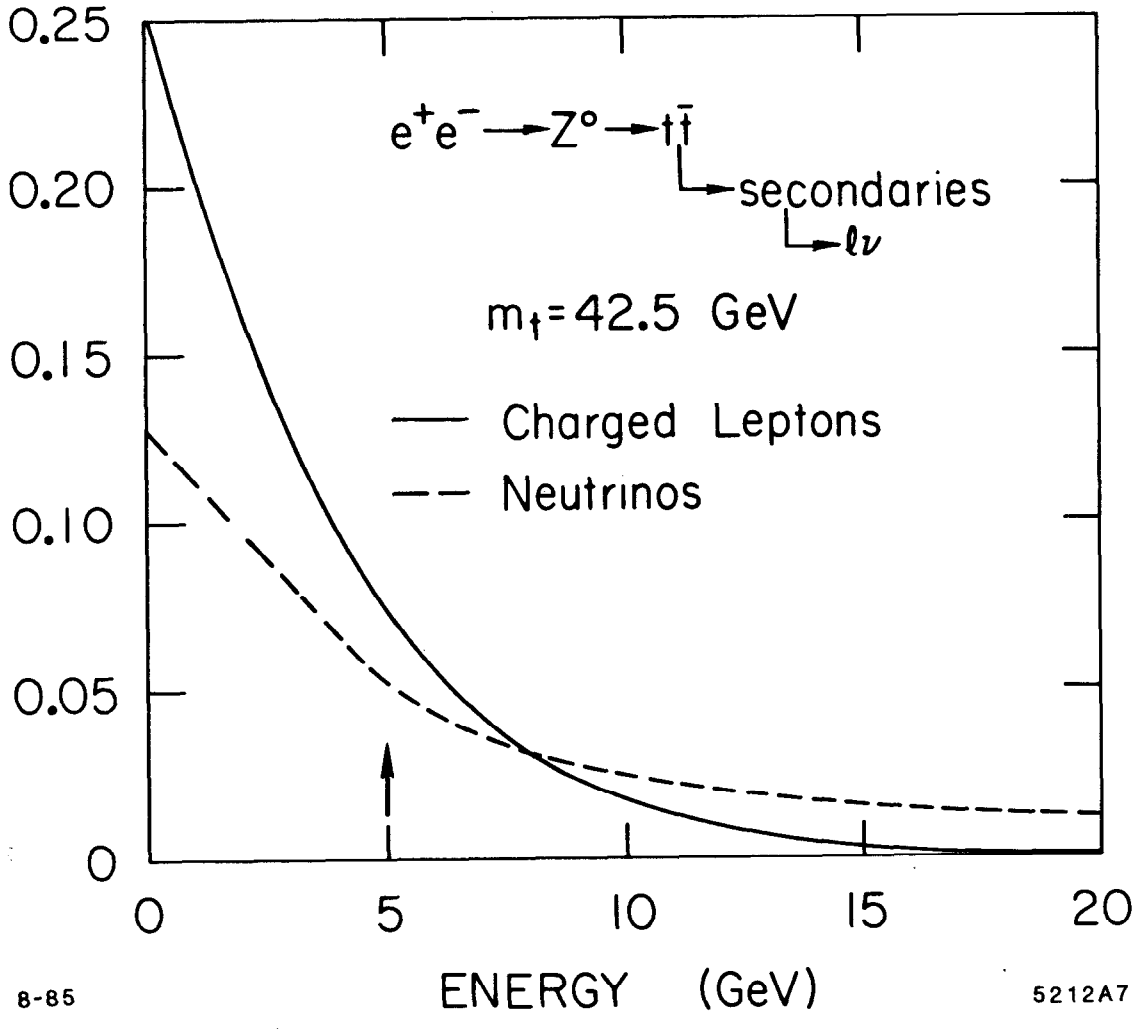
0.25
0.20
0.15
0.10
0.05
0
0
5
10
15
20
$e^+e^- \rightarrow Z^\circ \rightarrow t\bar{t}$
secondaries
$\ell\nu$
$m_t = 42.5$ GeV
Charged Leptons
Neutrinos
ENERGY (GeV)
8-85
5212A7

FIG. 5

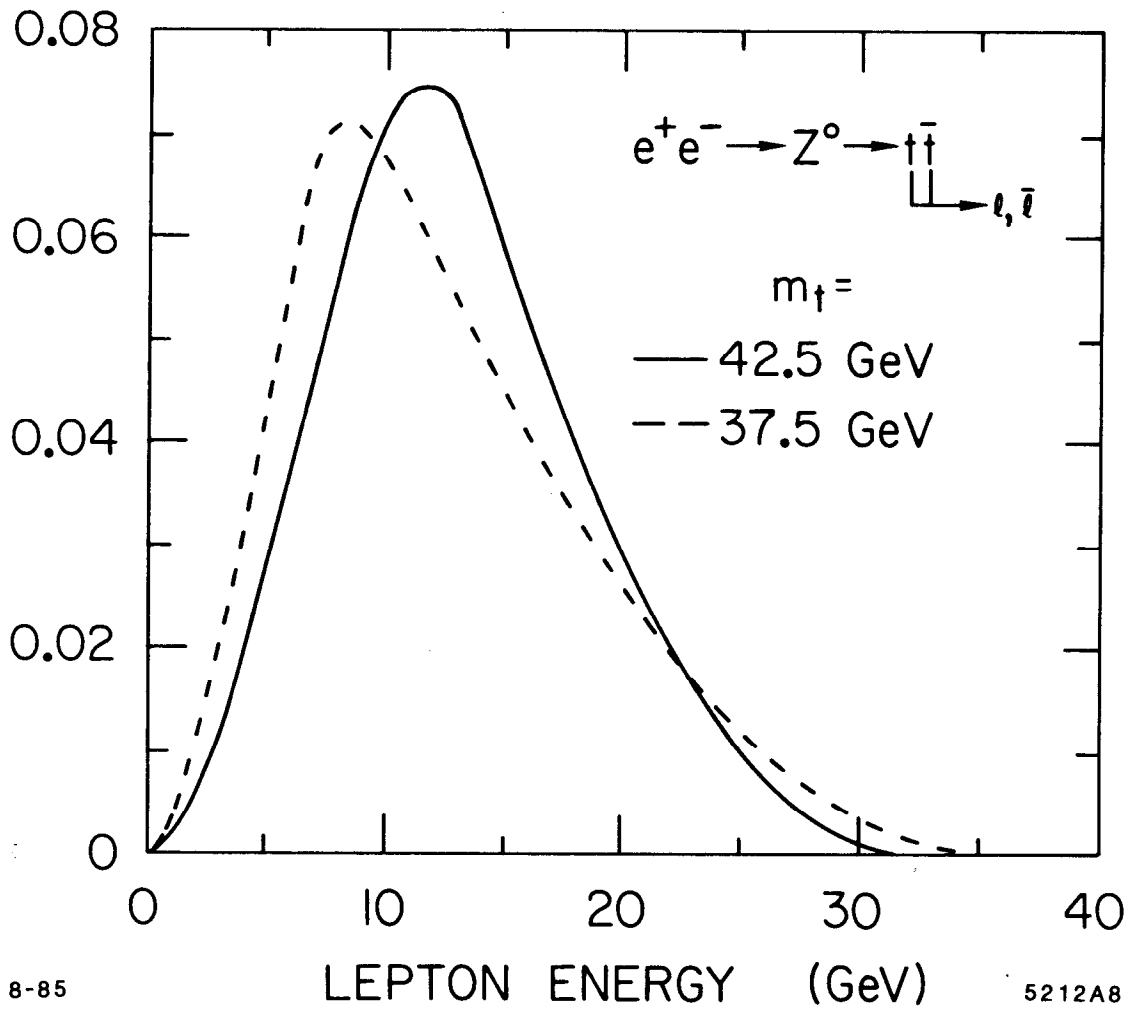
0.08
0.06
0.04
0.02
0
0
10
20
30
40
$e^+e^- \rightarrow Z^\circ \rightarrow t\bar{t}$
$\ell, \bar{\ell}$
m_t =
42.5 GeV
37.5 GeV
LEPTON ENERGY (GeV)
8-85
5212A8

FIG. 6A

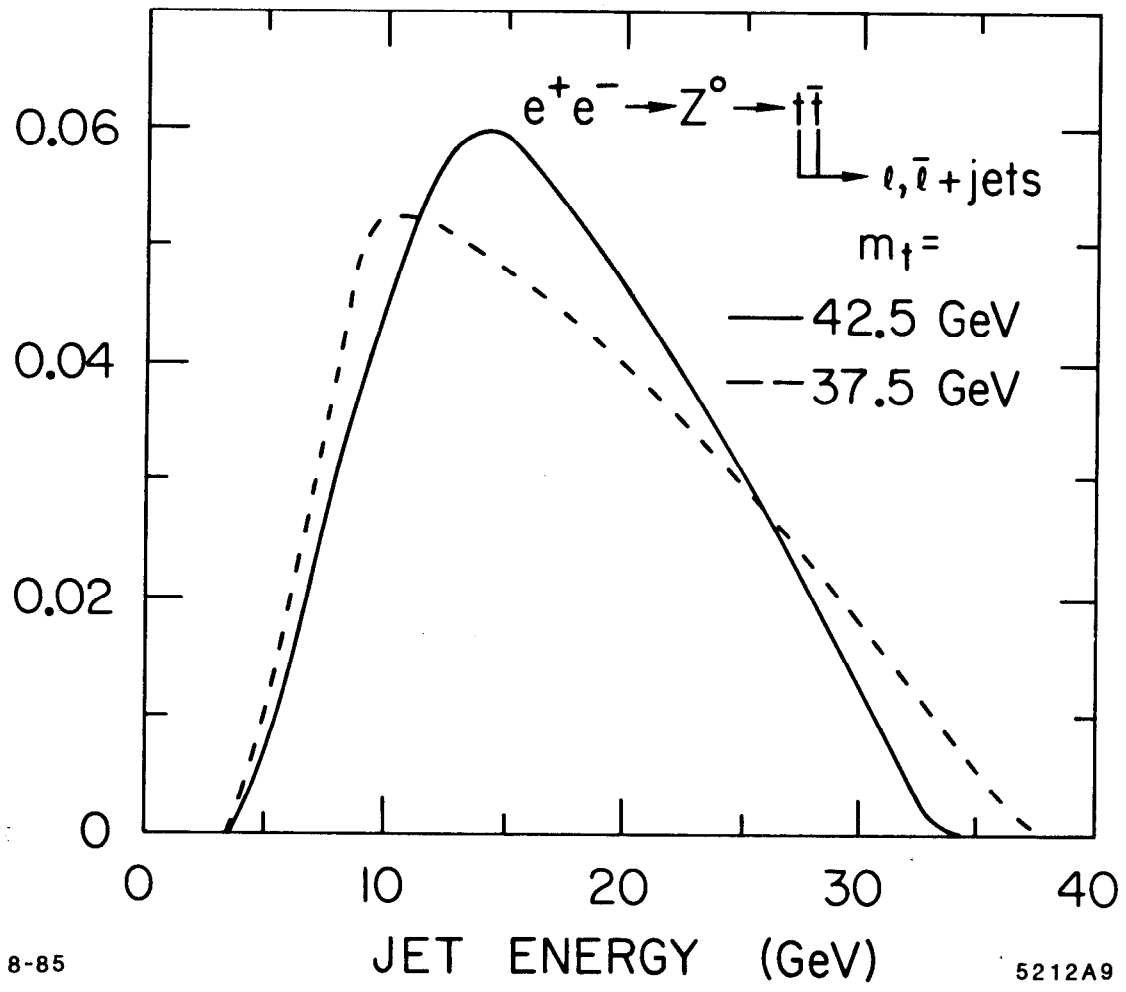
0.06
0.04
0.02
0
$e^+e^- \rightarrow Z^\circ \rightarrow t\bar{t}$
$\ell, \bar{\ell}$ + jets
m_t =
42.5 GeV
37.5 GeV
0
10
20
30
40
JET ENERGY (GeV)
8-85
5212A9

FIG. 6B

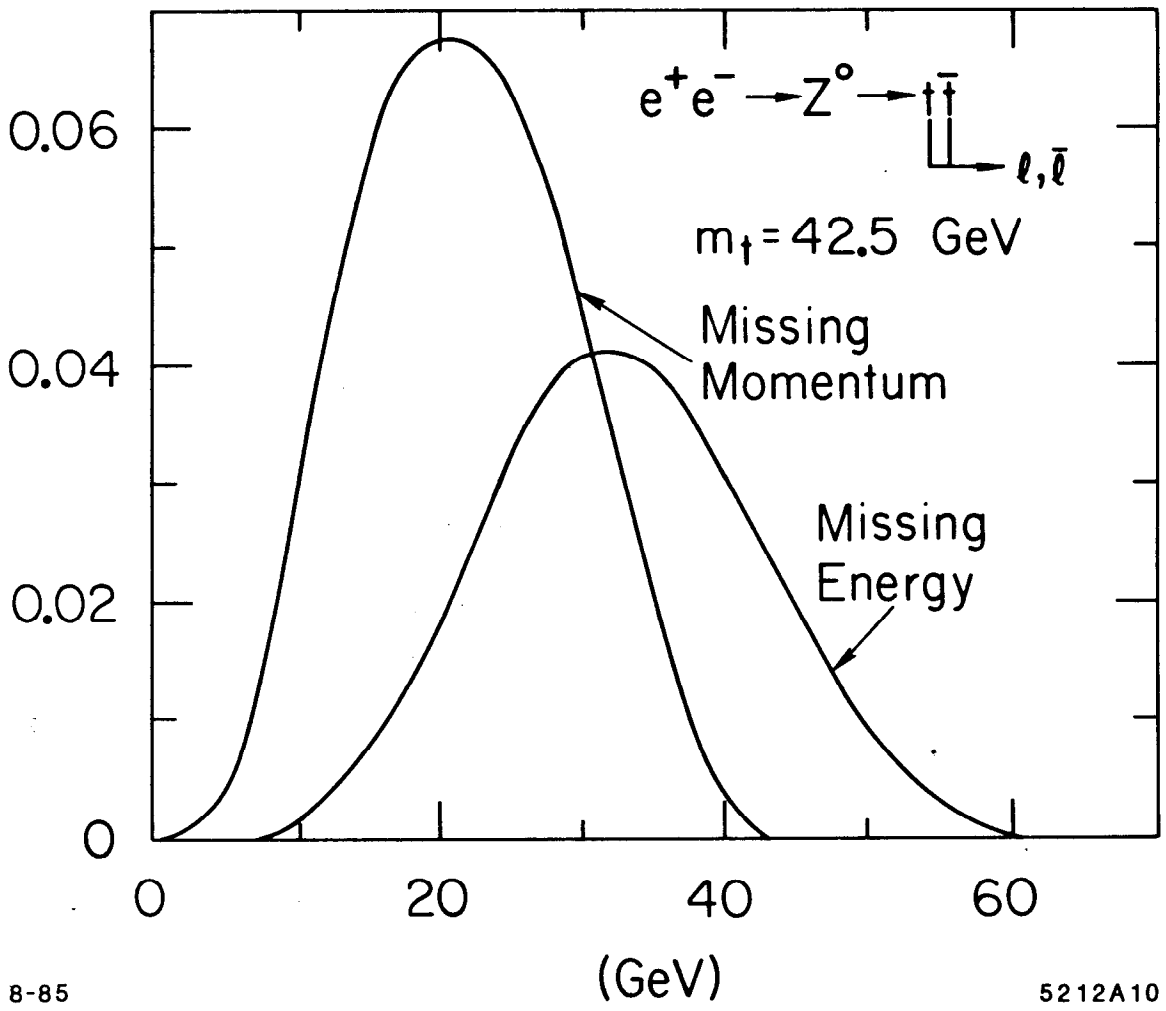
0.06
0.04
0.02
0
0
20
40
60
(GeV)
$e^+e^- \rightarrow Z^\circ \rightarrow t\bar{t}$
$\ell, \bar{\ell}$
$m_t = 42.5$ GeV
Missing Momentum
Missing Energy
8-85
5212A10

FIG. 6c

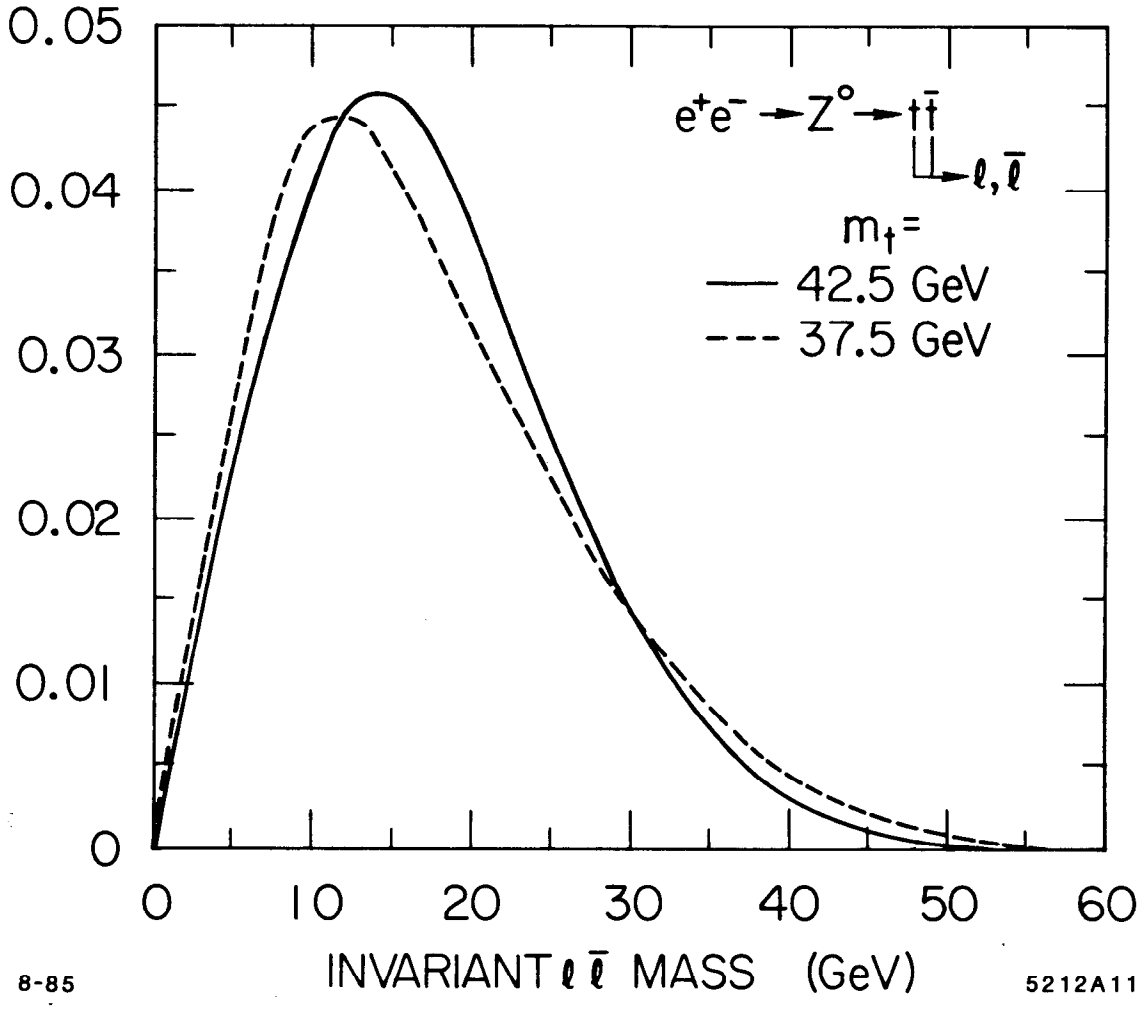
0.05
0.04
0.03
0.02
0.01
0
0
10
20
30
40
50
60
$e^+e^- \rightarrow Z^\circ \rightarrow t\bar{t}$
$\ell, \bar{\ell}$
m_t =
42.5 GeV
37.5 GeV
INVARIANT $\ell\bar{\ell}$ MASS (GeV)
8-85
5212A11

FIG. 6D

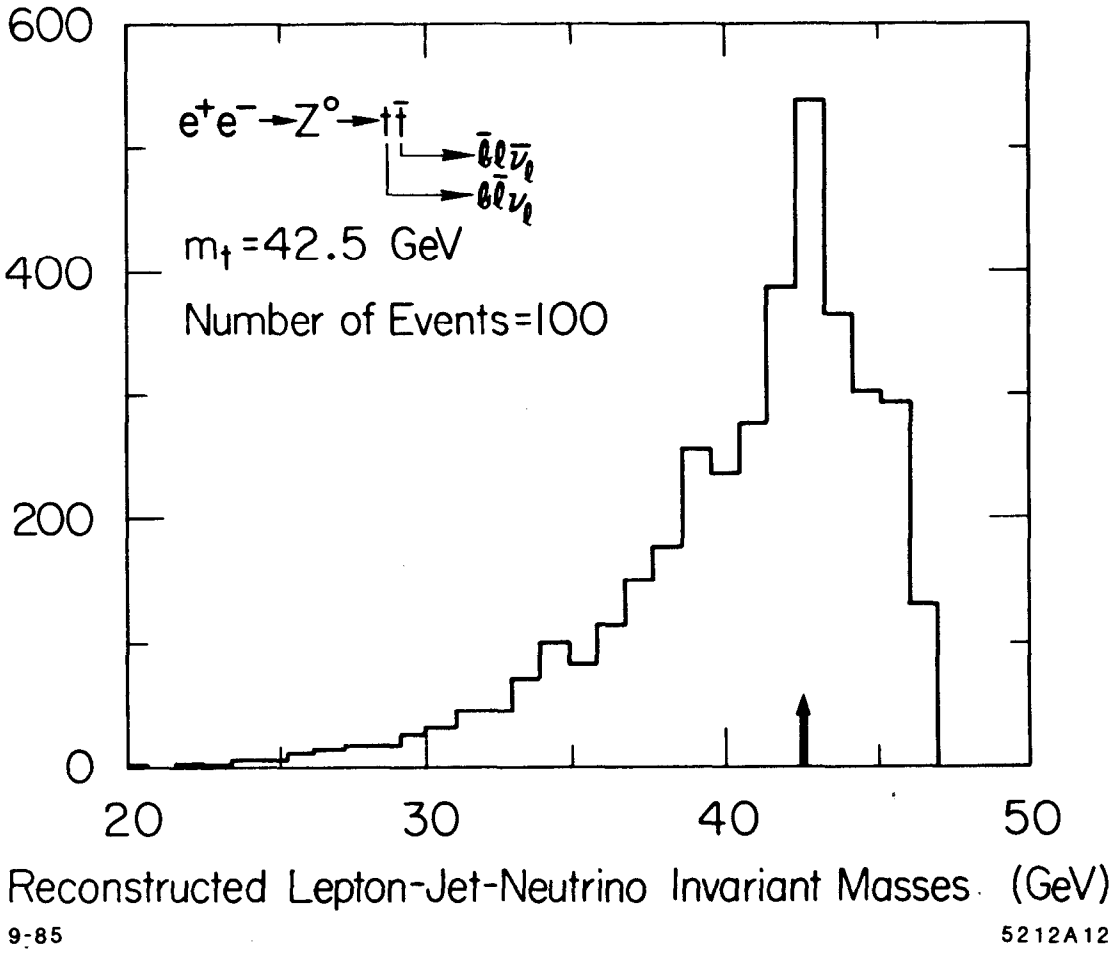
600
400
200
0
$e^+e^- \to Z^\circ \to t\bar{t}$
$\to b\ell\bar{\nu}_\ell$
$\to b\bar{\ell}\nu_\ell$
$m_t = 42.5$ GeV
Number of Events=100
20
30
40
50
Reconstructed Lepton-Jet-Neutrino Invariant Masses (GeV)
9-85
5212A12

FIG. 7

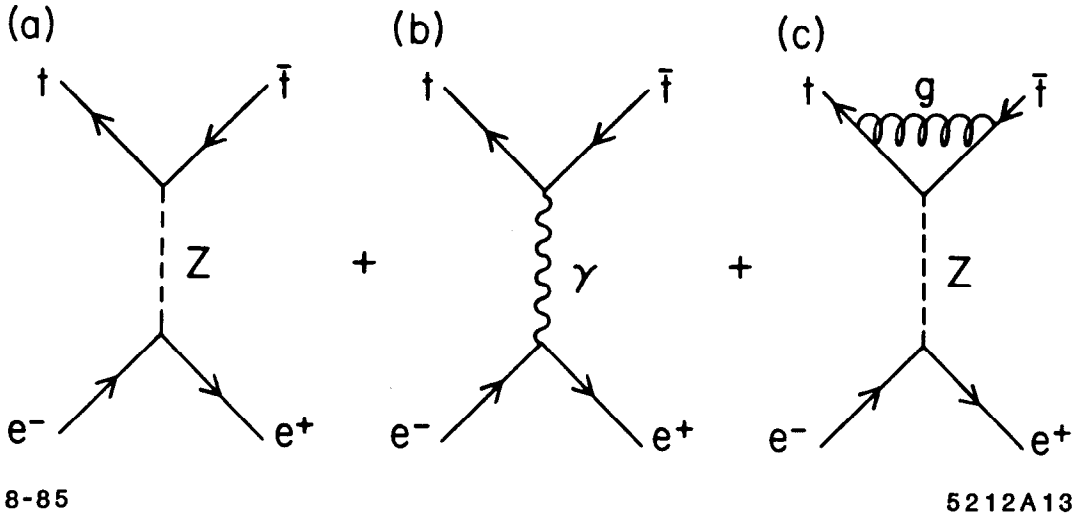

FIG. 8

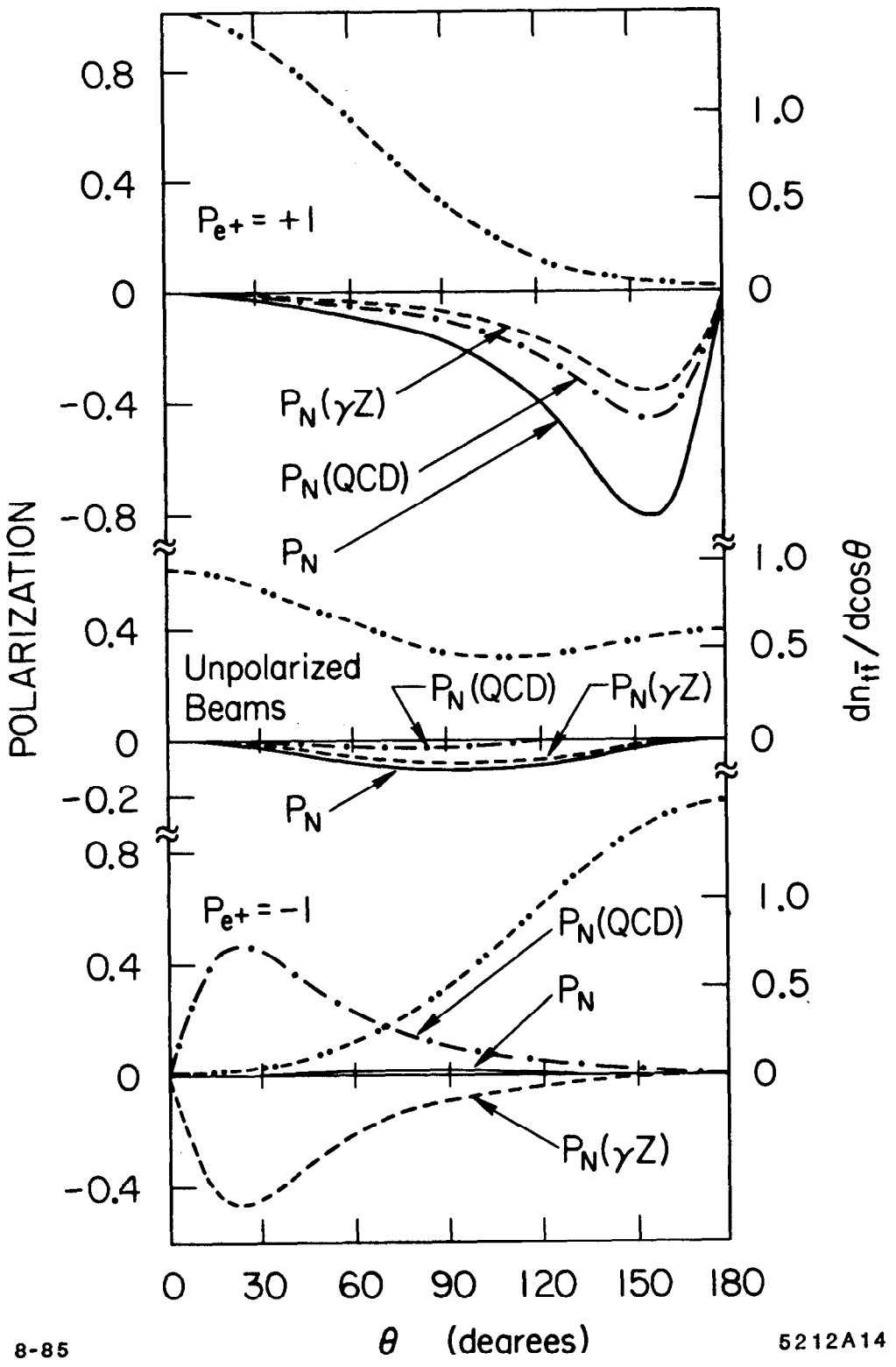
0.8
0.4
0
-0.4
-0.8
$P_{e+} = +1$
$P_N(\gamma Z)$
$P_N(QCD)$
P_N
1.0
0.5
0
0.4
0
-0.2
Unpolarized
Beams
$P_N(QCD)$
$P_N(\gamma Z)$
P_N
0.8
0.4
0
-0.4
$P_{e+} = -1$
$P_N(QCD)$
P_N
$P_N(\gamma Z)$
POLARIZATION
$d\sigma_{t\bar{t}}/d\cos\theta$
0
30
60
90
120
150
180
θ (degrees)
8-85
5212A14

FIG. 9